Progress In Electromagnetics Research M, Vol. 27, 191–201, 2012

A POLARIZATION-INDEPENDENT WIDE-ANGLE DUAL DIRECTIONAL ABSORPTION METAMATERIAL ABSORBER

Lei Lu[1, *], Shaobo Qu[1], Hua Ma[1], Fei Yu[1], Song Xia[2], Zhuo Xu[2], and Peng Bai[3]

[1]College of Science, Air Force Engineering University, Xi'an 710051, China

[2]Electronic Materials Research Laboratory, Key Laboratory of the Ministry of Education, Xi'an Jiaotong University, Xi'an 710049, China

[3]Synthetic Electronic Information System Research Department, Air Force Engineering University, Xi'an 710051, China

Abstract—In this paper, a polarization-independent wide-angle planar metamaterial absorber exhibiting dual directional absorption is proposed. Measurement results indicate that the planar metamaterial absorber achieves absorptivities of 86.87% and 91.48% to the normally incident electromagnetic waves propagating in forward $(+z)$ and backward $(-z)$ directions, respectively. Due to geometry's fourfold rotational symmetry, the absorber is polarization-independent. Additionally, the absorber works well for a wide range of incident angles for both transverse electric and transverse magnetic polarizations. Besides its impressing performance, this planar metamaterial absorber is also extremely thin that it's thickness is approximately 1/32 of the working wavelength.

1. INTRODUCTION

Presently, with perfect absorption and ultra-thin thickness metamaterial absorber has attracted great attention worldwide. In 2008, N. I. Landy et al. [1] firstly demonstrated a perfect experimental metamaterial absorber composed of an electric ring resonator over a cut wire which were separated by a lossy dielectric substrate. The electric response derives from the electric ring resonator, on the other hand,

Received 21 October 2011, Accepted 22 November 2012, Scheduled 26 November 2012

* Corresponding author: Lei Lu (bblfdd@163.com).

the magnetic response is aroused by antiparallel currents in the cut wire and the center wire of the electric ring resonator. From then on, metamaterial absorbers operating at microwave [2–5], terahertz [6–10], infrared [11–16], and optical [17–19] frequencies have been widely researched. However, most of the metamateiral absorbers mentioned above are asymmetric in wave propagation direction, therefore, these absorbers have high absorption in one direction while little absorption in opposite direction. S. Gu et al. [20] proposed a low-reflection two-dimensional metamaterial absorber based on lumped elements. Although this absorber can absorb waves in two directions normal to its surface, its polarization dependence as well as lumped elements make the fabrication complicated. C. G. Hu et al. [21] proposed a dual directional absorption planar metamaterial absorber. The magnetic resonance of the absorber achieves simultaneous dropping in transmission and reflection at terahertz frequency, however, it is also polarization dependent.

A polarization-independent wide-angle dual directional planar metamaterial absorber is designed, simulated and measured in this paper. The planar metamaterial absorber with extremely thin thickness which is just about 1/32 of the working wavelength is comparatively easy to realize.

2. DESIGN AND SIMULATION

The proposed metamaterial absorber is composed of a doubly periodic array of face-coupled pairs of Jerusalem cross and split square ring

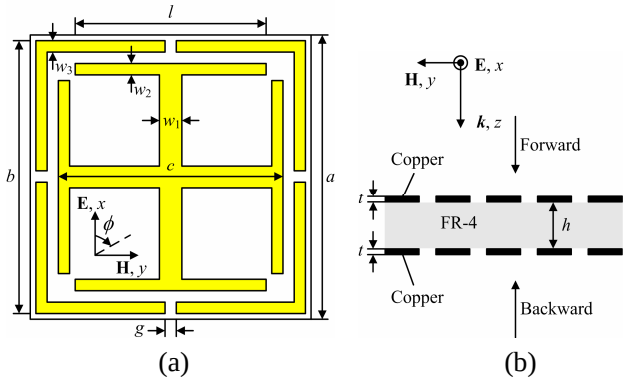

Figure 1. Schematic and geometry of the metamaterial absorber. (a) Unit cell and (b) side view.

shaped conductors. A unit cell of the metamaterial absorber is shown in Figure 1(a). Owing to the unit cell's rotational symmetry, this metamaterial absorber provides a two-dimensional isotropic response to any linearly polarized incident wave. The conductors are made of copper with the thickness $t = 20\,\mu\text{m}$ and electric conductivity $\sigma = 5.8 \times 10^7\,\text{S/m}$ printed on opposite sides of a FR-4 dielectric substrate with the relative permittivity $\varepsilon_r = 4$, the loss tangent 0.025, and the thickness $h = 0.8\,\text{mm}$. Other dimensions are $a = 5\,\text{mm}$, $b = 4.8\,\text{mm}$, $c = 4\,\text{mm}$, $l = 3.4\,\text{mm}$, $w_1 = 0.4\,\text{mm}$, $w_2 = w_3 = 0.2\,\text{mm}$, $g = 0.2\,\text{mm}$.

The metamaterial absorber is simulated with a commercial frequency-domain electromagnetics solver, CST Microwave Studio. Perfect electric conductor (PEC) and perfect magnetic conductor (PMC) boundary conditions are placed in x and y directions to model a periodic array of the unit cell. Figure 1(b) shows the polarization of normally incident electromagnetic waves propagating in forward $(+z)$ and backward $(-z)$ directions. Reflection R and Transmission T are obtained from the frequency-dependent S-parameter S_{11} and S_{21} ($R = |S_{11}|^2$ and $T = |S_{21}|^2$). The absorption is calculated as $A = 1 - R - T$.

Figure 2 shows the simulation results of the metamaterial absorber. Since the metamaterial absorber is symmetric in wave propagation directions, the forward (along the $+z$ direction) reflection and transmission are the same as backward (along the $-z$ direction) results, Figure 2 only shows the simulated reflection, transmission, and absorption of the metamaterial absorber under $+z$ direction incident wave. The reflection as well as the transmission have declined to their minimum simultaneously at 11.15 GHz. This brings about a peak absorption of 92.7%.

To confirm the polarization-independent feature of the proposed metamaterial absorber, the absorptive characteristic has been analyzed under normal incident plane waves with various electric field polarizations. The polarization angle ϕ is defined as the angle between electric field ($\mathbf{E}$) and x-axis as shown by the inset in Figure 1(a). The simulated results of different polarization angles are shown in Figure 3. Due to the fourfold rotational symmetry of the geometry, the magnitude and frequency of the peak absorption are both nearly invariant as the ϕ increases from 0° to 90°. Therefore, the proposed metamterial absorber is insensitive to the polarization angle of the normal incident wave.

To better understand the nature of the proposed metamaterial absorber, the current distribution at peak absorption frequency 11.15 GHz is shown in Figure 4. It clearly displays that the antiparallel

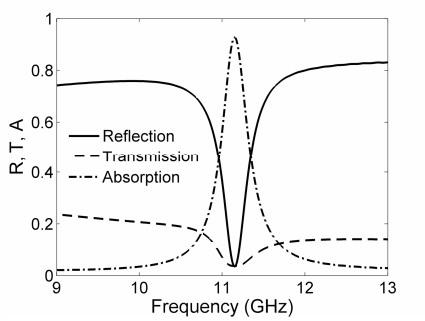

Figure 2. Simulated reflection, transmission, and absorption of the metamaterial absorber.

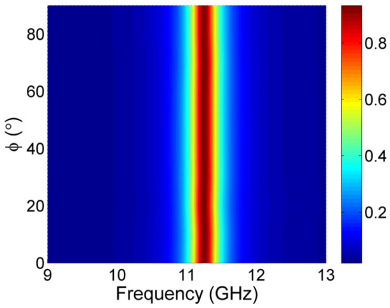

Figure 3. Simulated absorption for different polarization angles for the normal incidence.

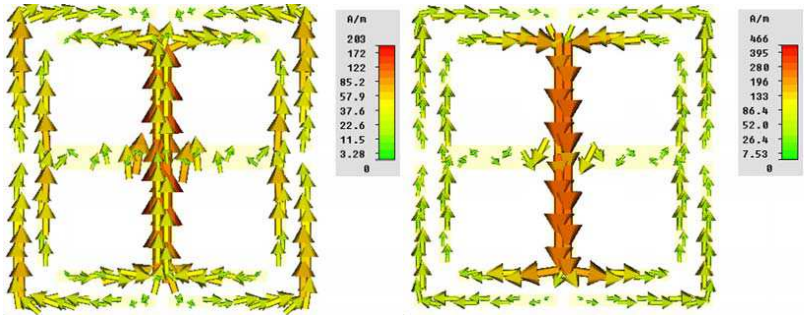

Figure 4. The surface current distribution on (a) top and (b) bottom metallic structures of the metamaterial absorber at 11.15 GHz.

currents are primarily concentrated on the central parts of Jerusalem cross shaped conductors. The antiparallel currents give rise to a magnetic resonance. The metamaterial absorber also exhibits electric resonance due to the excitation of co-directional currents on the pair of split square rings. At this frequency, the strength of the magnetic resonance overwhelms the electric resonance, and thus the high absorption can be attributed to the magnetic response of the structure.

Moreover, simulation results of absorption expressed by a function of frequency and incident angle in transverse electric (TE) and transverse magnetic (TM) polarizations has been presented in Figure 5. Under the condition of TM polarization, the absorption peak is nearly independent of the incident angle and achieves 90% even at 70°. This

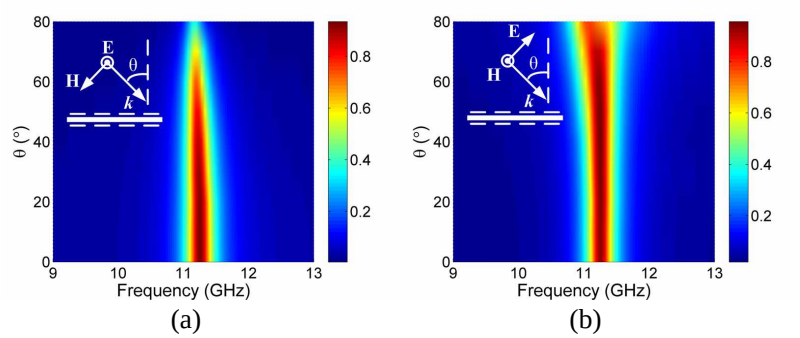

Figure 5. Contour plot of the simulated absorption as a function of frequency and angle of incidence under (a) TE and (b) TM polarizations.

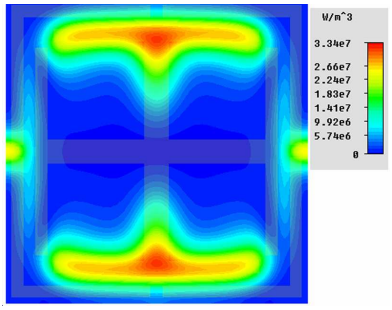

Figure 6. The distribution of the power loss density for the metamaterial absorber at 11.15 GHz.

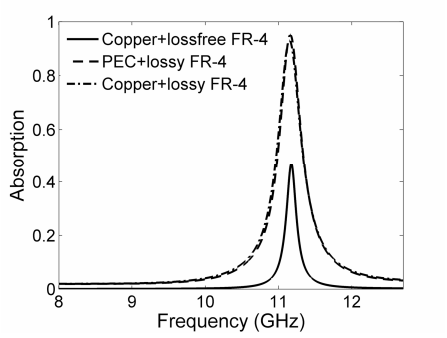

Figure 7. Absorption for different material properties of the metal layers and the dielectric layer.

is because the direction of the incident wave's magnetic field remains unchanged with various incident angles and it can efficiently drive the circulating currents at all incident angles. However, the magnetic field cannot drive the circulating currents efficiently at large angles [7] under TE polarization. Eventhough, the absorption still achieves 60% at 70°. As the simulation results reveal, the metamaterial absorber performs well under both TE and TM polarizations over a wide range of incident angles.

To better the comprehension of the physical insight, Figure 6 shows the distribution of the power loss density at the peak absorption frequency of the metamaterial absorber. As shown in Figure 6, the

strong power loss is mainly focused on the two arms of the Jerusalem cross which is primarily caused by the strong magnetic coupling.

Absorption for different material properties of metal layers and dielectric layer is shown in Figure 7. The copper and lossfree FR-4 achieve a absorptivity of 46.77%. The PEC and lossy FR-4 nearly achieve the perfect absorption of the copper and lossy FR-4. Consequently, high absorption is mainly generated by the dielectric loss of FR-4 dielectric substrate rather than the Ohmic loss of metal patterns.

To further study the resonant behavior of the proposed metamaterial absorber, real and imaginary parts of both retrieved surface electric susceptibility and magnetic susceptibility denoted as χ_{es} and χ_{ms} respectively [22–24] have been demonstrated in Figure 8 (assuming $e^{i\omega t}$ time dependence). For a TE polarization normal incident plane wave, the two surface susceptibilities are determined by

$$\chi_{es} = -\frac{2i}{k_0}\frac{1-r-t}{1+r+t} \tag{1}$$

$$\chi_{ms} = -\frac{2i}{k_0}\frac{1+r-t}{1-r+t} \tag{2}$$

where r and t are the reflection and transmission coefficients at normal incidence, and k_0 is the wave number in free space. Metasurface, also called single-layer metamaterial, is defined as a periodic two-dimensional structure, of which the thickness and periodicity are small compared with the wavelength in the surrounding media [24]. Since a metasurface does not have a well-defined thickness, appropriate and unique parameters to characterize the metasurface are surface

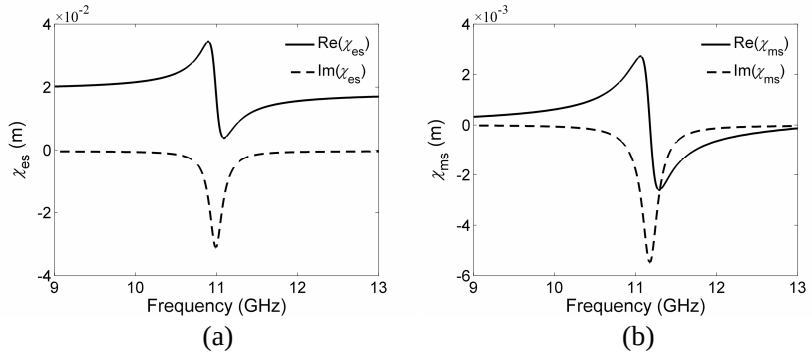

Figure 8. Surface susceptibilities for the metamaterial absorber. (a) χ_{es} and (b) χ_{ms}.

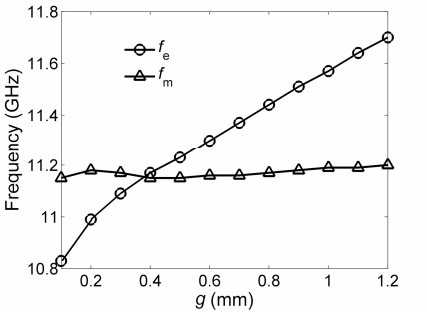

Figure 9. The dependence of the magnetic resonance frequency f_m and the electric resonance frequency f_e on the gap g of the split square ring.

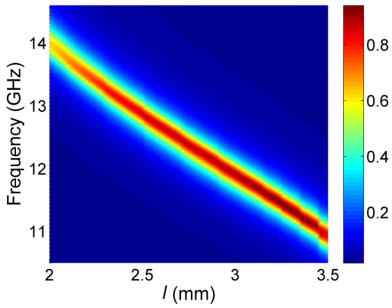

Figure 10. The dependence of the absorption on the length l of the Jerusalem cross arm.

susceptibilities. This retrieval approach has no needs to choose the appropriate sign of a square root, nor require the assumption of an arbitrary layer thickness. It can also be applied to a bilayer metamaterial [25]. In Figure 8, an electric resonance as well as a magnetic resonance occur at frequencies of $f_e = 10.99\,\text{GHz}$ and $f_m = 11.18\,\text{GHz}$, respectively. This further demonstrates that the peak absorption at 11.15 GHz is mainly aroused by magnetic resonance.

The dependence of both magnetic resonance frequency f_m and electric resonance frequency f_e on the split square ring's gap g has been shown in Figure 9. Simulation results demonstrate that f_e is rather sensitive to the gap g while f_m is independent of g. By varying the gap g, the electric resonance can be tuned very carefully and moved to the magnetic resonance frequency, which can makes the metamaterial absorber impedance-matched to the free space and obtain large losses due to the strong resonance. This causes that both reflection and transmission achieve their minimum simultaneously as shown in Figure 2.

The dependence of absorption on Jerusalem cross arm's length denoted as l has been plotted in Figure 10. As l increases from 2 mm to 3.5 mm, the peak absorption frequency decreases. Further, the absorption still remains greater than 80% with a length l larger than 2.3 mm. Simulation results in Figure 10 demonstrate that both magnetic and electric resonance shift towards lower frequencies with a larger length l.

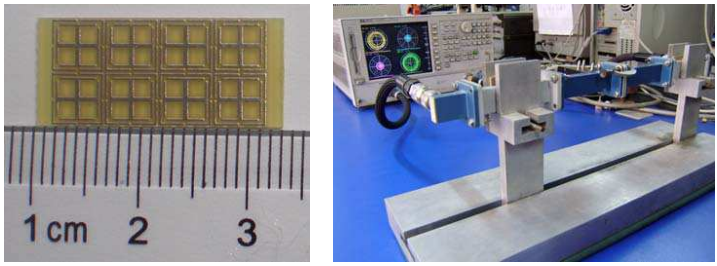

(a) (b)

Figure 11. (a) Photograph of the fabricated metamaterial absorber sample. (b) The X-band rectangular waveguide and vector network analyzer.

3. FABRICATION AND MEASUREMENT

In this paper, we used rectangular waveguide test system to verify the absorption. This method can detect all reflected and transmitted waves so as to obtain the absorption of normal incidence. The waveguide method only needs to test a small scale metamaterial absorber sample, and the test system is also simple. The proposed metamaterial absorber sample designed according to Figure 1 is realized with standard printed circuit board technology. A photograph of the sample (4×2 unit cell sample with 22.8 mm $\times$ 10.1 mm) is shown in Figure 11(a). The measurement system shown in Figure 11(b) is composed of a standard X-band rectangular waveguide BJ100 and an HP8720ES vector network analyzer.

The rectangular waveguide test system can only measure the reflection and transmission of the sample for normal incident TE polarization electromagnetic wave, and due to the fourfold rotational symmetry of the sample unit cell, S parameters of both normal incident TE and TM polarizations electromagnetic waves are the same, so we just need to test the sample under normal incident TE polarization electromagnetic wave. The measured reflection, transmission and absorption of the metamaterial absorber with incident waves along the forward ($+z$) and backward ($-z$) directions are plotted in Figure 12. The forward and backward reflections are minimized at 11.08 GHz simultaneously. Both of the forward and backward transmission curves are nearly the same and get the minimum at the same frequency 11.08 GHz. The peak absorption values of the forward and backward normal incident waves are 86.87% and 91.48% respectively. The measured results agree well with simulation data and verify the dual

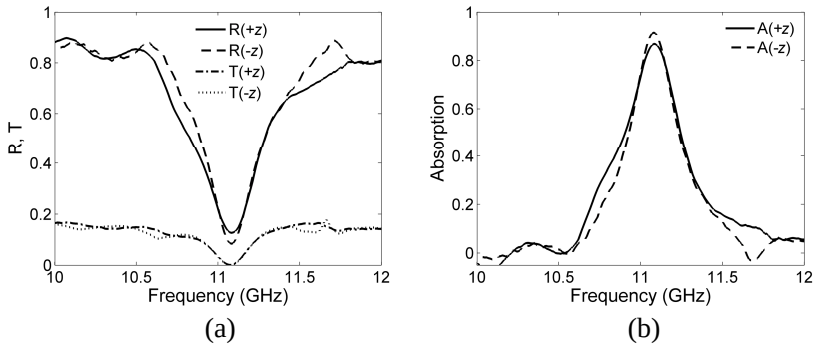

Figure 12. Measured (a) reflection, transmission, and (b) absorption for an incident wave along the forward $(+z)$ and backward $(-z)$ directions through the metamaterial absorber.

directional absorption of the proposed metamaterial absorber. The redshift of the peak absorption frequency compared with simulation results is mainly caused by fabrication tolerance. The overall thickness of the metamaterial absorber is only 0.84 mm which is approximately 1/32 of the working wavelength.

4. CONCLUSION

In conclusion, a polarization-independent dual directional absorption planar metamaterial absorber has been designed, simulated as well as fabricated in this paper. Experimental measurements demonstrate the dual directional absorption of the metamaterial absorber. The thickness of the planar metamaterial absorber is ultra-thin that it is approximately 1/32 of the working wavelength. This metamaterial absorber has many advantages such as simple design, strong practicability and bright application foreground.

ACKNOWLEDGMENT

This work was supported partly by the Nation Basic Research Program of China under Grant No. 2009CB623306, and partly supported by the National Natural Science Foundation of China (Grant Nos. 11274389, 61071058, and 11204378).

REFERENCES

1. Landy, N. I., S. Sajuyigbe, J. J. Mock, D. R. Smith, and W. J. Padilla, "Perfect metamaterial absorber," *Physical Review Letters*, Vol. 100, 207402, 2008.
2. Li, M. H., H. L. Yang, X. W. Hou, Y. Tian, and D. Y. Hou, "Perfect metamaterial absorber with dual bands," *Progress In Electromagnetics Research*, Vol. 108, 37–49, 2010.
3. Xu, Y. Q., P. H. Zhou, H. B. Zhang, L. Chen, and L. J. Deng, "A wide-angle planar metamaterial absorber based on split ring resonator coupling," *Journal of Applied Physics*, Vol. 110, 044102, 2011.
4. Li, L., Y. Yang, and C. Liang, "A wide-angle polarization-insensitive ultra-thin metamaterial absorber with three resonant modes," *Journal of Applied Physics*, Vol. 110, 063702, 2011.
5. Huang, L. and H. Chen, "Multi-band and polarization insensitive metamaterial absorber," *Progress In Electromagnetics Research*, Vol. 113, 103–110, 2011.
6. Tao, H., N. I. Landy, C. M. Bingham, X. Zhang, R. D. Averitt, and W. J. Padilla, "A metamaterial absorber for the terahertz regime: Design, fabrication and characterization," *Optics Express*, Vol. 16, 7181–7188, 2008.
7. Tao, H., C. M. Bingham, A. C. Strikwerda, D. Pilon, D. Shrekenhamer, N. I. Landy, K. Fan, X. Zhang, W. J. Padilla, and R. D. Averitt, "Highly flexible wide angle of incidence terahertz metamaterial absorber: Design, fabrication, and characterization," *Physical Review B*, Vol. 78, 241103(R), 2008.
8. Landy, N. I., C. M. Bingham, T. Tyler, N. Jokerst, D. R. Smith, and W. J. Padilla, "Design, theory, and measurement of a polarization-insensitive absorber for terahertz imaging," *Physical Review B*, Vol. 79, 125104, 2009.
9. Grant, J., Y. Ma, S. Saha, L. B. Lok, A. Khalid, and D. R. S. Cumming, "Polarization insensitive terahertz metamaterial absorber," *Optics Letters*, Vol. 36, 1524–1526, 2011.
10. Huang, L., D. R. Chowdhury, S. Ramani, M. T. Reiten, S.-N. Luo, A. J. Taylor, and H.-T. Chen, "Experimental demonstration of terahertz metamaterial absorbers with a broad and flat high absorption band," *Optics Letters*, Vol. 37, 154–156, 2012.
11. Avitzour, Y., Y. A. Urzhumov, and G. Shvets, "Wide-angle infrared absorber based on a negative-index plasmonic metamaterial," *Physical Review B*, Vol. 79, 045131, 2009.
12. Liu, N., M. Mesch, T. Weiss, M. Hentschel, and H. Giessen,

"Infrared perfect absorber and its application as plasmonic sensor," *Nano Letters*, Vol. 10, 2342–2348, 2010.

13. Liu, X. L., T. Starr, A. F. Starr, and W. J. Padilla, "Infrared spatial and frequency selective metamaterial with near-unity absorbance," *Physical Review Letters*, Vol. 104, 207403, 2010.
14. Jiang, Z. H., S. Yun, F. Toor, D. H. Werner, and T. S. Mayer, "Conformal dual-band near-perfectly absorbing mid-infrared metamaterial coating," *Acs Nano*, Vol. 5, 4641–4647, 2011.
15. Feng, Q., M. B. Pu, C. G. Hu, and X. G. Luo, "Engineering the dispersion of metamaterial surface for broadband infrared absorption," *Optics Letters*, Vol. 37, 2133–2135, 2012.
16. Dayal, G. and S. A. Ramakrishna, "Design of highly absorbing metamaterials for infrared frequencies," *Optics Express*, Vol. 20, 17503–17508, 2012.
17. Aydin, K., V. E. Ferry, R. M. Briggs, and H. A. Atwater, "Broadband polarization-independent resonant light absorption using ultrathin plasmonic super absorbers," *Nature Communications*, Vol. 2, 517, 2011.
18. Wang, Y., T. Y. Sun, T. Paudel, Y. Zhang, Z. F. Ren, and K. Kempa, "Metamaterial-plasmonic absorber structure for high efficiency amorphous silicon solar cells," *Nano Letters*, Vol. 12, 440–445, 2012.
19. Wang, J. Q., C. Z. Fan, P. Ding, J. N. He, Y. G. Cheng, W. Q. Hu, G. W. Cai, E. J. Liang, and Q. Z. Xue, "Tunable broad-band perfect absorber by exciting of multiple plasmon resonances at optical frequency," *Optics Express*, Vol. 20, 14871–14878, 2012.
20. Gu, S., J. P. Barrett, T. H. Hand, B. I. Popa, and S. A. Cummer, "A broadband low-reflection metamaterial absorber," *Journal of Applied Physics*, Vol. 108, 064913, 2010.
21. Hu, C., X. Li, Q. Feng, X. N. Chen, and X. Luo, "Introducing dipole-like resonance into magnetic resonance to realize simultaneous drop in transmission and reflection at terahertz frequency," *Journal of Applied Physics*, Vol. 108, 053103, 2010.
22. Holloway, C. L., A. Dienstfrey, E. F. Kuester, J. F. O'Hara, A. K. Azad, and A. J. Taylor, "A discussion on the interpretation and characterization of metafilms/metasurfaces: The two-dimensional equivalent of metamaterials," *Metamaterials*, Vol. 3, 100–112, 2009.
23. Holloway, C. L., E. F. Kuester, and A. Dienstfrey, "Characterizing metasurfaces/metafilms: The connection between surface suscep-

tibilities and effective material properties," *IEEE Antennas and Wireless Propagation Letters*, Vol. 10, 1507–1511, 2011.

24. Holloway, C. L., E. F. Kuester, J. A. Gordon, J. O'Hara, J. Booth, and D. R. Smith, "An overview of the theory and applications of metasurfaces: The two-dimensional equivalents of metamaterials," *IEEE Antennas and Propagation Magazine*, Vol. 54, 10–35, 2012.
25. Morits, D. and C. Simovski, "Electromagnetic characterization of planar and bulk metamaterials: A theoretical study," *Physical Review B*, Vol. 82, 165114, 2010.